RESPONSES OF A FLOATING OFFSHORE WIND TURBINE WITH RC FLOATERS SUBJECTED TO SHIP COLLISION LOADS

Yanyan Sha, Yuping Zhong, and Bo Wang

Department of Mechanical and Structural Engineering and Materials Science, University of Stavanger, Stavanger, Norway

Abstract

Wind energy has enormous potential in reducing greenhouse emissions and curbing global warming. The number of installed offshore wind turbines has been continuously growing worldwide in recent years. Most offshore wind farms are located near the coast and close to the main shipping routes, thus are under the risk of accidental collisions by passing ships causing possible casualties and economic losses. Therefore, it is essential to understand the response of offshore wind turbines and properly design them against ship collisions. Several studies have been reported on ship collisions with wind turbines with fixed foundations. However, limited analyses have been conducted for ship collisions with floating offshore wind turbines (FOWTs). In this paper, the ship collision response of a FOWT with reinforced concrete (RC) semisubmersible foundation is investigated. A two-step ship-FOWT collision analysis framework is proposed with first evaluating the local structural deformation and a following analysis of global structural motion and internal force. In this paper, emphasis is placed on the local structural response of the RC floater using the nonlinear finite element code LS-DYNA. Parametric studies are conducted to study the effect of impact velocity, impact location, and strain rate. The force-displacement curves obtained from the local simulations can then be utilized to further evaluate the global responses of the FOWT.

Keywords: ship collision, floating offshore wind turbine, concrete, structural damage

1. INTRODUCTION

Wind energy, as one of the renewable energy sources with enormous potential, plays a key role against global warming and counterbalances greenhouse gas emissions. According to the International Energy Agency, offshore wind electricity production increased rapidly in recent years, with an increase of 32% in 2017 and 20% in 2018, and it is expected to increase to 606 TWh by 2030 [1]. The total installed offshore wind capacity in Europe is now more than 25 GW, and 116 offshore wind farms across 12 countries have been grid-connected [2]. With the development of floating wind turbine technology, larger offshore wind turbines are designed and constructed further into the ocean.

Onshore wind turbine usually has a limited size due to limitations in installation space and blade transportation. Visual and noise issues also limit the further development of onshore wind turbine. The average wind speed onshore is also generally smaller than the wind speed offshore which result in smaller electricity productions. Compared with onshore wind turbines, offshore wind turbines have greater wind speed and larger size. Offshore wind turbines can be categorized as grounded and floating systems. The floating systems, such as semi-submersible, spar-buoy, tension leg platforms, are mainly used when the water depth is larger than 60 m. Most of the floaters of FOWTs are made of steel due to a lighter total material weight and relatively constant material property compared to concrete. However, reinforced concrete floaters have also been proposed for several concepts. Compared with steel structures, RC structures has outstanding characteristics such as corrosion resistance, simple construction, and low cost. One example of the FOWTs with RC floaters is the OO-Star wind floater as shown in Figure 1 [3].

Figure 1. The OO-Star wind floater [3].

As offshore wind farms are usually located near the coast and shipping routes, they are under the risk of accidental ship collisions. The collision consequences of the wind turbines can be significant, including power outrage, structural failures, and possible human injuries and fatalities. Therefore, it is of vital importance to design the FOWTs against ship collision loads. The collision mechanics of ship collision with offshore installations have been widely studied since 1980s. Amdahl [4] investigated the collisions between offshore supply vessels and platforms. Energy dissipation mechanisms of various ship structural components subjected to collision loads are formulated. Pedersen and Zhang [5] studied ship collisions with ships, rigid walls, and flexible offshore structures. Analytical expressions were proposed for estimation of energy dissipation and maximum impact force. In the past decade, some analyses were also reported for ship collision with wind turbines. Bela et al. [6] investigated the response of an offshore wind turbine with monopile foundations impacted by a ship where the wind turbine response under the collision of both rigid and deformable ship bows are simulated. It was found that a deformable ship bow only induced deformation in the wind turbine is only half of that when impacted by a rigid ship bow. Marquez et al. [7] investigated the accuracy of three concrete constitutive material models in LS-DYNA for modelling flexural and shear failure of RC wind turbine foundations when subjecting to rigid ship bow collisions. In general, previous studies focused on the collision analysis of wind turbines with steel substructures. The collision response of wind turbines with RC foundations, especially floating RC foundations, has not been well investigated.

In this paper, a two-step decoupled approach is introduced for ship-FOWT collision analyses. Both local and global responses of the FOWTs can be obtained. The emphasis of this paper is placed on the local collision response of a pontoon in the floater. Numerical simulations were conducted to study the effect of impact velocity, impact location, and strain rate. The numerical model of the global analysis is also briefly introduced.

2. METHODOLOGY

During a collision event, the bow, side, or stern of the striking ship will collide with the floaters of the FOWT which float at sea level. The floaters may be subjected to local deformations should the collision demand exceed the design capacity of the floaters. Meanwhile, the struck FOWT will also move due to the large kinetic energy of the striking ship which may further induce excessive motion and internal forces in the supporting tower. To obtain a comprehensive evaluation of the responses of a FOWT under ship collisions, both the local structural and global kinetic responses shall be included. Two approaches, i.e., coupled analysis and decoupled two ways, are normally used for analyzing ship collision with ships and floating structures. In the decoupled analysis, the local and global responses are considered in two separate analyses. For the local analysis, a prescribed motion or an initial velocity can be assigned to the ship structure which collides into the FOWT. The force-deformation curves obtained in the local

analysis can then be used in the global analysis to analyze the motion and internal forces of the FOWT. In the coupled analysis, the motions of both the ship and the FOWT will be calculated based on hydrodynamic forces by potential theory also considering the inertia and collision forces. The coupled method is generally very time-consuming and thus is seldom used. The decoupled method, on the other hand, has been used for analyzing the collision responses of floating bridges [8] and floating fish farms [9]. In this study, the decoupled approach is also used where the analysis is split into two parts, i.e. evaluating the local response of the pontoon segment using LS-DYNA and obtaining the global response analysis of the whole FOWT using OrcaFlex. The emphasis of this paper is placed on the first part while the second part is briefly introduced.

3. FINITE ELEMENT MODELS

4.1 FOWT

Various types of steel and reinforced concrete floaters have been designed for FOWTs. In this study, a recently proposed OO-Star wind floater for supporting floating wind turbines is shown in Figure 2. The floater includes 3 outer columns, a central column, a star-shaped pontoon, and a bottom slab. The columns are supported by the pontoon while the slab is attached to the bottom of the pontoon. The detailed dimensions of the platform are illustrated in the figure.

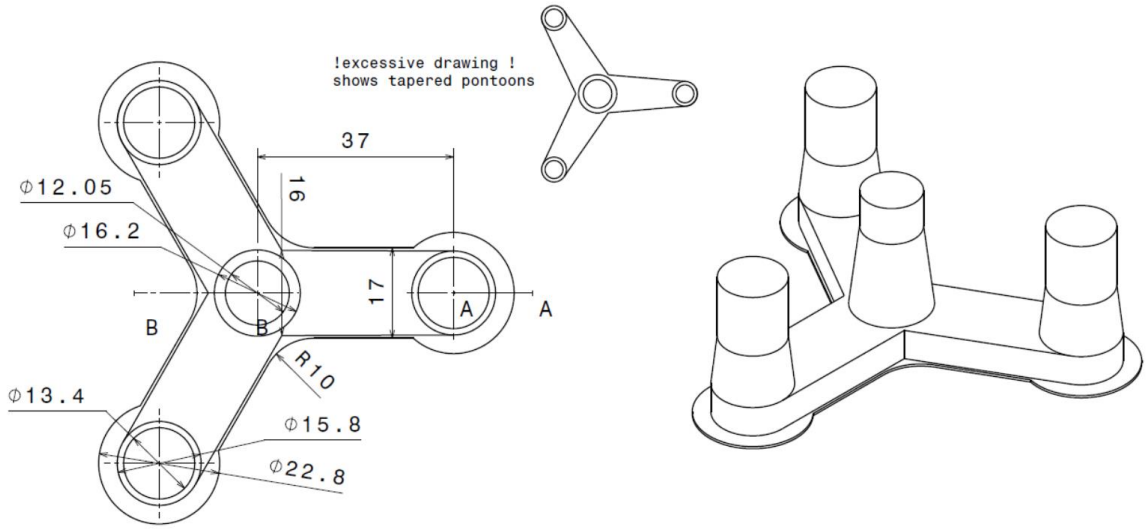

Figure 2. Main dimensions of the OO-Star wind floater [10].

Based on the structural dimensions in Figure 2, a finite element model of the half pontoon is developed as shown in Figure 3(a). The total height of the pontoon is 24.5 m with a top straight part and an oblique bottom part as illustrated in the figure. The internal diameters in the top and the bottom part are 13.4 m and 15.4 m respectively. As detailed information regarding the floater design is not available, a thickness of 1 m is selected for the pontoon wall based on the previous study [11]. The steel reinforcement dimension and layout of the pontoon is designed according to calculations following the design code. Two layers of steel rebars are arranged close to the outer and inner surface of the pontoon wall as shown in Figure 3(a). The diameters of the longitudinal and transverse reinforcement are 40 mm and 24 mm respectively. For the outer layer of reinforcements, the longitudinal rebars have a spacing of 173 mm while the transverse rebars are spaced at a 200 mm distance. The spacings for the inner longitudinal and transverse rebars are 150 mm and 200 mm respectively. Solid elements were used to model the concrete while beam elements were utilized to model the steel reinforcements. The coupling between the reinforcement and the concrete is considered by the keyword *CONSTRAINED_LAGRANGE_IN_SOLID in LS-DYNA.

4.2 Ship bow

A ship model bow model is developed based on a container ship with 20,000-ton displacement as shown in Figure 3(b). The ship bow consists of the bulbous bow and a forecastle with a draught of 9.6 m. Both the outer ship hull and the internal decks, frames, bulkheads, stringers, and stiffeners were also carefully modelled according to the design drawing [12]. Four-node Belytschko-Lin-Tsay shell elements were used when modelling the various structural components in the ship bow. The thicknesses of the panels and stiffeners are in the range of 7.5 mm to 20.5 mm. The general element size is 80 mm. In the simulation, an added mass of 10% is considered for the head-on collision scenarios.

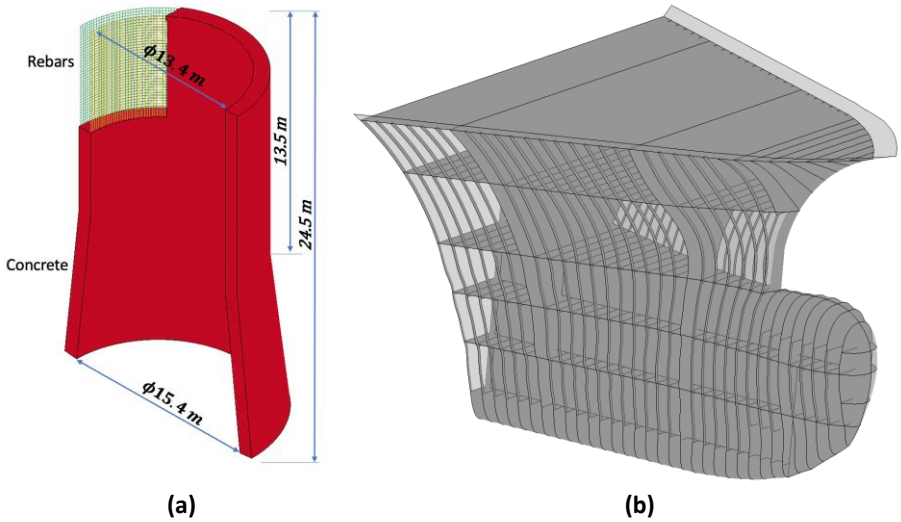

Figure 3. Finite element (FE) models of (a) the column floater, and (b) the ship.

4.3 Material modelling

In this study, C60 grade concrete which is commonly used for offshore structures is selected for the concrete in the floater. The concrete material is modelled by *MAT_CONCRETE_DAMAGE_REL3 in LS-DYNA. This material model has been proved to be able to accurately simulate the damage of concrete under impact and collision loads [13]. The steels used for the reinforcement in the floater and the ship are B500c and S275 respectively. The material model *MAT_PIECEWISE_LINEAR_PLASTICITY is used for both the reinforcements and the ship bow. The key parameters for the concrete and steel materials are listed in Table 1.

Table 1. Material properties of the steel and concrete.

Material	LS-DYNA material model	Parameter	Value
Steel reinforcement	*MAT_PIECEWISE_LINEAR_PLASTICITY	Density	7850 kg/m^3
		Young's modulus	200 GPa
		Poisson's ratio	0.3
		Yield strength	580 MPa
Concrete	*MAT_CONCRETE_DAMAGE_REL3	Density	2400 kg/m^3
		Poisson's ratio	0.2
		Compressive strength	60 MPa
Steel in ship bow	*MAT_PIECEWISE_LINEAR_PLASTICITY	Density	7800 kg/m^3
		Young's modulus	200 GPa
		Poisson's ratio	0.3
		Yield strength	275 MPa

4. LOCAL RESPONSE

With the established local model of the RC floater and the ship bow, parametric numerical simulations were conducted. In the simulation, various initial velocities were assigned to the ship bow colliding

with the pontoon at different locations. The strain rate effect is also investigated. In all local simulations, the pontoon was fixed through the nodes at the rear surface.

4.1 Effect of impact velocity

Ships navigating in open sea waters normally travel at a speed of 10-20 knots (ca 5-10 m/s). In this study, three impact velocities, i.e., 2. 5 m/s, 5 m/s, and 10 m/s were selected to investigate the effect of impact velocity on the collision response. Figure 4 shows the impact force-time histories for both the ship bulb and the forecastle impact with the pontoon at the three velocities. It can be seen from the figure that the maximum impact force increases as the impact velocity increases. In all three cases, the pontoon has limited deformation while excessive damage occurs in the ship bow. Figure 5 shows the snapshots of the pontoon damage under the ship bow impact with a velocity of 10 m/s. High plastic strain regions are limited within the small contact area in the early phase. As the ship crushes further, high plastic strain regions expand, however, no element failure occurs in the pontoon. For the ship bow, both the bulb and the forecastle endure increasing deformation as the ship crushes further into the pontoon as shown in Figure 6. The impact force level is thus dominated by the strength of the ship bow. The structural responses are similar for smaller impact velocities of 2.5 m/s and 5 m/s.

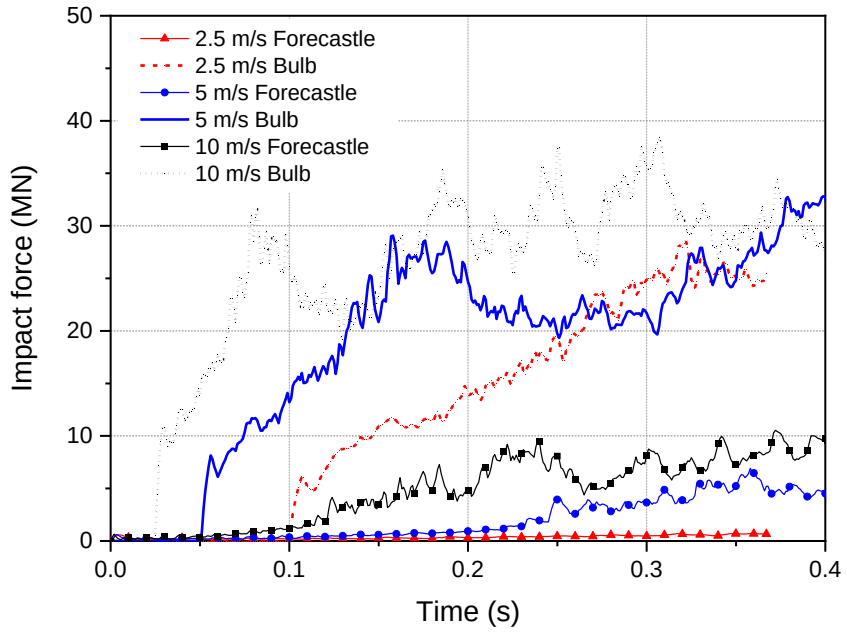

Figure 4. Impact force-time histories for different impact velocities.

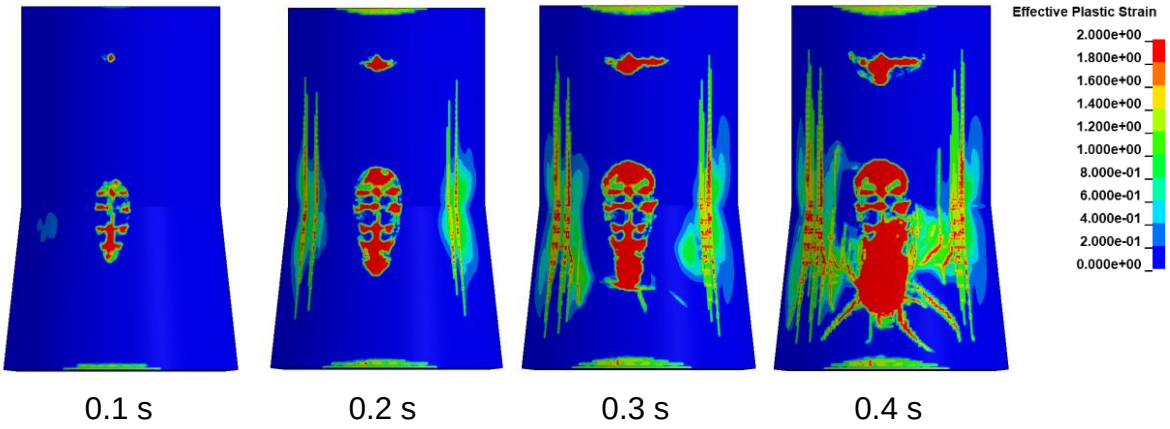

Figure 5. Pontoon damage at different time instant for 10 m/s collision scenario

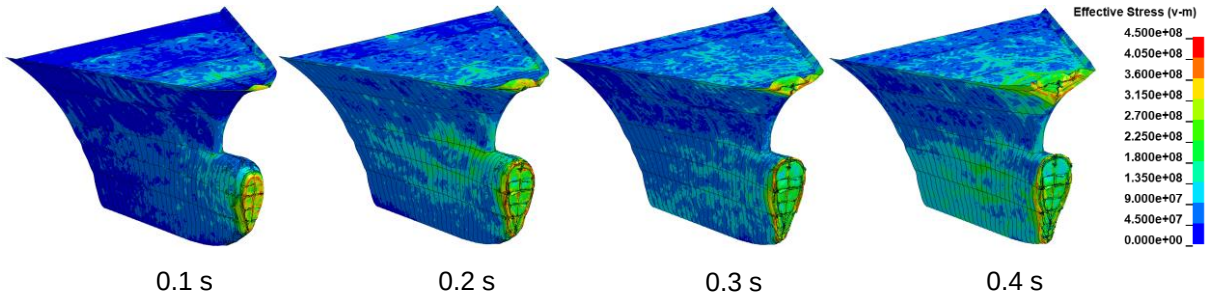

Figure 6. Ship bow damage at different time instant for 10 m/s collision scenario

4.2 Effect of impact location

During a collision accident, the ship can collide with the pontoon at any locations. To investigate the effect of different impact locations, numerical simulations were also conducted for an impact at 2 m away from the pontoon centre as illustrated in Figure 7(a). The impact force-time histories are compared with that of the central impact. Figure 7(b) shows that the impact force of forecastle-pontoon interaction is insensitive to the impact location. However, the impact force due to bulb impact dropped significantly after 0.2 s as shown in the figure. This is because the ship was deflected away from the pontoon with a sliding motion. This can be observed in the bulb damage evolvement as shown in Figure 8. Therefore, the impact location can significantly affect the collision process and consequently lead to different failure modes. The impact force and energy dissipation will also vary should the impact location change. This also applies to impact at the same location but with different impact angles.

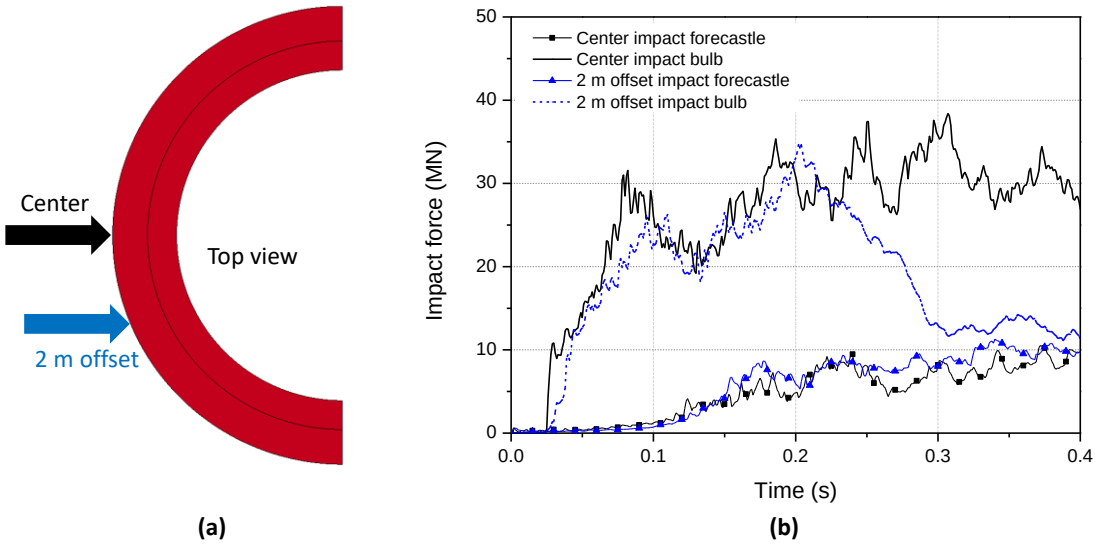

Figure 7. (a) Impact locations and (b) impact force-time histories for different collision scenarios with an impact velocity of 10m/s

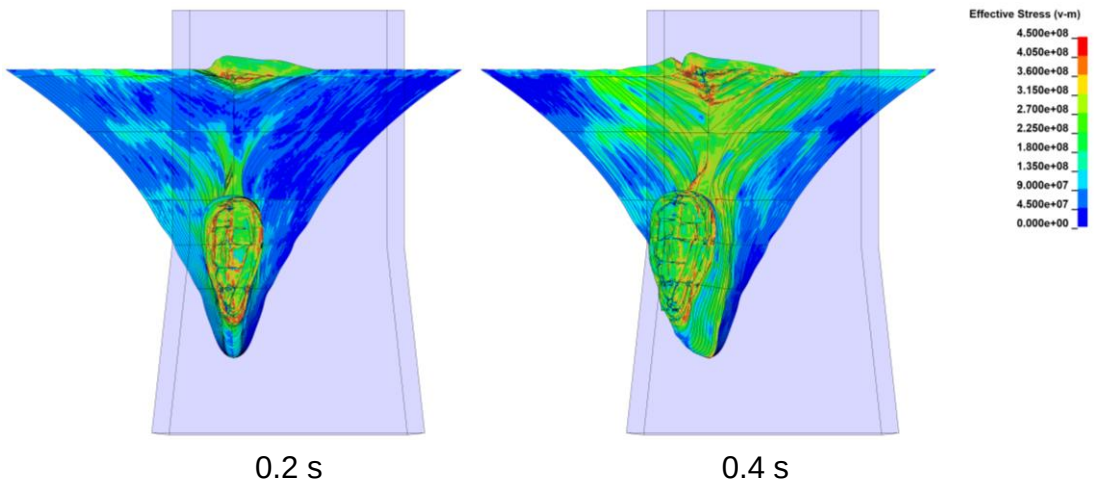

Figure 8. Ship bow damage at different time instant for 10 m/s collisions with an offset of 2 m.

4.3 Effect of strain rate

The concrete and steel materials are strain rate dependent when subjected to impact or collision loads. The strength of both materials can be significantly enhanced under high strain rates. However, for ship collisions when the impact speed is relatively low, the effect of strain rate is debatable. In this study, the strain rate effect is discussed by comparing the structural response with and without including the strain rate in the striking ship bow. The strain rate effect is considered by a dynamic increase factor (DIF) as described in Sha and Hao [14].

Figure 9 compares the impact force-time histories for 10 m/s collisions with and without considering the strain rate effect in the ship bow. It is observed that the strain rate effect is significant for the mild steel used in the ship bow. The peak impact force is much higher when the strain rate is included in the steel material for the ship bow. The ship bow is able to penetrate the pontoon wall when the strain rate is considered for the ship bow as the impact force plunged after 0.1 s. The structural responses are also compared in Figure 10. The ship bow endures large deformation while the pontoon is generally intact when strain rate is ignored. However, when strain rate is included in the steel material in the ship bow, the structural damage in the ship bow is significantly reduced while the pontoon was penetrated by the ship bow. It should be noted that only the strain rate effect of the striking ship bow is considered in the simulation which is the most conservative assumption. When the strain rate effect is also addressed for the concrete and steel reinforcement in the pontoon, the damage in the pontoon may be reduced. A more comprehensive investigation of the effect of the strain rate is necessary.

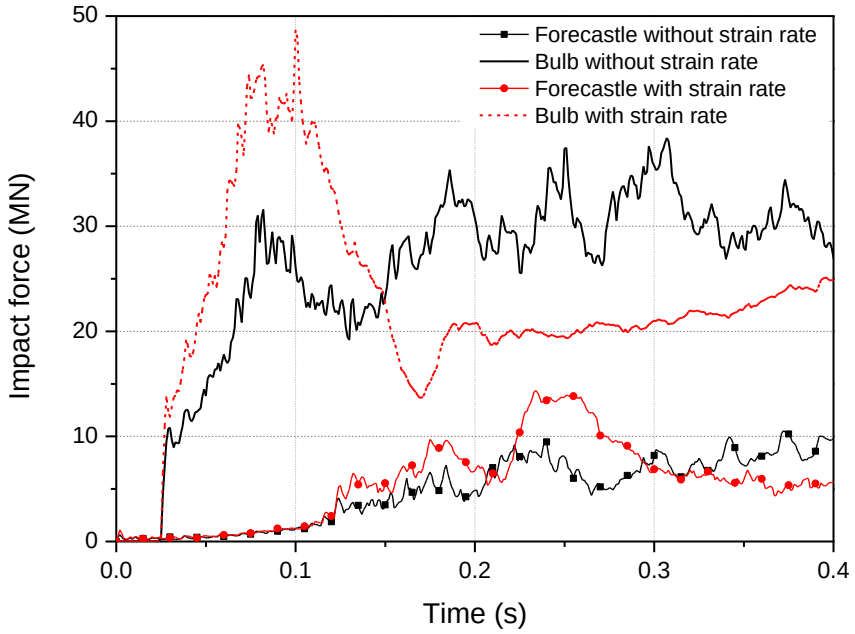

Figure 9. Impact force-time histories with and without considering the strain rate effect in the ship bow for 10 m/s collisions.

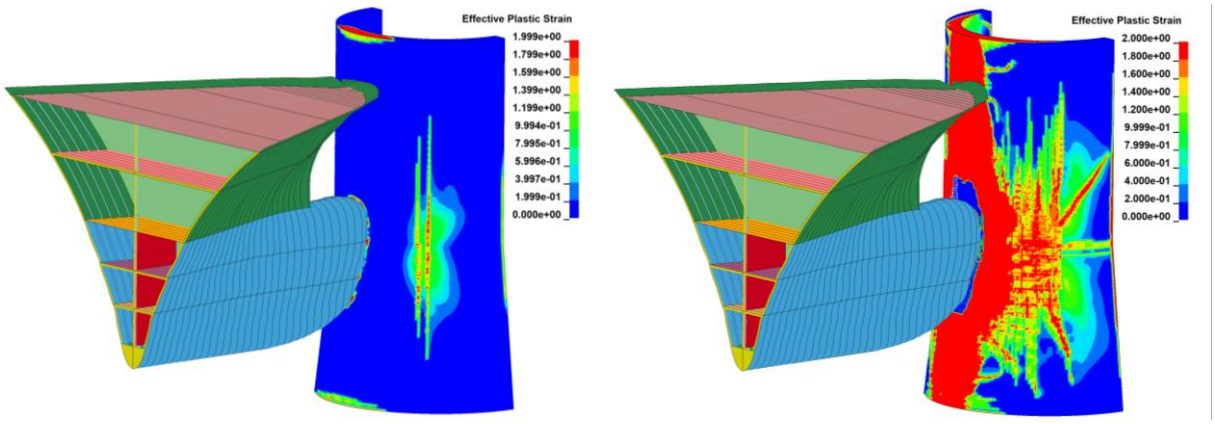

Figure 10. Structural damage for simulations with and without considering the strain rate effect in the ship bow for 10 m/s collisions.

5. GLOBAL RESPONSE

A comprehensive ship collision analysis with FOWT includes both local and global responses. For the decoupled approach used in this study, the local structural response is investigated in the above sections. The force-deformation curves obtained from local analyses can then be used as the spring stiffness in the global analysis. Both the hydrodynamic and aerodynamic responses will also be included in the global analysis in OrcaFlex. In the global analysis, various collision scenarios can be investigated by utilizing the corresponding force-deformation curves from the local analyses. Figure 11 shows an example setup for a head-on impact in one of the pontoons in the FOWT. The motion of the FOWT as well as the internal forces and moments of the tower and blades can be obtained both in the parked and operating conditions. These global responses will be reported in the future studies.

Figure 11. Global ship-FOWT collision analysis setup

6. CONCLUSIONS

This paper presents a case study of ship collision with a semi-submersible floating wind turbine with a reinforced concrete floater. The following conclusions can be drawn from the study:

- The magnitude of the impact force depends on the impact velocity of the striking ship. A larger impact speed will lead to a higher impact force.
- For the proposed structural design of the pontoon with 1 m thickness, it is able to resist the impact from the container ship bow. Major structural damage occurs in the ship bow which dissipates the majority of the collision energy. The pontoon wall has limited deformation in the early phase, but the damage can accumulate as the ship crushes further.
- Impact location can have a significant effect on the structural response. The ship bow may experience sliding motion and thus be drifted away from the pontoon. This will lead to a shorter impact duration and less severe damage in the pontoon.
- The strain rate effect may change the collision behaviour of the ship bow and the pontoon completely. The ship bow deformation dominates when the strain rate is not included. However, the ship bow penetrated the pontoon when the strain rate effect is included for the ship bow. Further analysis is required to fully understand the effect of the strain rate for both the ship bow and the RC pontoon at different impact velocities.

Acknowledgement

The simulations were performed on resources provided by Sigma2 - the National Infrastructure for High Performance Computing and Data Storage in Norway (project number NN9721K). This support is greatly acknowledged by the authors.

References

1. Kamran, M. and M.R. Fazal, Fundamentals of renewable energy systems. Renewable energy conversion systems, 2021: p. 1.
2. Deveci, M., E. Özcan, and R. John. Offshore wind farms: A fuzzy approach to site selection in a black sea region. in 2020 IEEE Texas Power and Energy Conference (TPEC). 2020. IEEE.
3. GL, L.B.D., Qualification of innovative floating substructures for 10MW wind turbines and water depths greater than 50m. 2015.

4. Amdahl, J., Energy absorption in ship-platform impacts. 1983.
5. Pedersen, P.T. and S.J.M.S. Zhang, On impact mechanics in ship collisions. 1998. 11(10): p. 429-449.
6. Bela, A., et al., Ship collision analysis on offshore wind turbine monopile foundations. 2017. 51: p. 220-241.
7. Márquez, L., P. Rigo, and H. Le Sourne. Ship collision events against reinforced concrete offshore structures. in Developments in the Analysis and Design of Marine Structures: Proceedings of the 8th International Conference on Marine Structures (MARSTRUCT 2021, 7-9 June 2021, Trondheim, Norway). 2021. CRC Press.
8. Sha, Y., J. Amdahl, and C. Dørum, Local and global responses of a floating bridge under ship-girder collisions. Journal of Offshore Mechanics and Arctic Engineering, 2018.
9. Yu, Z., et al., Numerical analysis of local and global responses of an offshore fish farm subjected to ship impacts. 2019. 194: p. 106653.
10. Yu, W., et al., Public Definition of the Two LIFES50+ 10MW Floater Concepts. 2017. 4.
11. Sha, Y., CFRP strengthening of reinforced concrete pontoon walls against ship bow collisions. Structure and Infrastructure Engineering, 2020: p. 1-16.
12. Sha, Y. and J. Amdahl, Numerical investigations of a prestressed pontoon wall subjected to ship collision loads. Ocean Engineering, 2019. 172: p. 234-244.
13. Sha, Y. and H. Hao, Nonlinear finite element analysis of barge collision with a single bridge pier. Engineering Structures, 2012. 41: p. 63-76.
14. Sha, Y. and H. Hao, Laboratory tests and numerical simulations of CFRP strengthened RC pier subjected to barge impact load. International Journal of Structural Stability and Dynamics, 2015. 15(02): p. 1450037.